

Resonances in ^{10}He and the $6n$ system studied using SAMURAI

O.Nasr^{1,*}, D.Beaumel^{1,5,**}, P.J.Li^{2,3,4,***}, L. Achouri⁶, M. Assié¹, T. Aumann^{11,12}, H. Baba⁵, G. Cardella¹³, S. Ceruti¹⁴, S. Chen⁴, A. Corsi¹⁷, S. Franchoo¹, A. Frotscher¹¹, J. Gao¹⁸, J. Gibelin⁶, A. Gillibert¹⁷, V. Girard-Alcindor¹, F. Hammache¹, T. Harada⁵, K. Inaba¹⁹, T. Isobe⁵, T. Kawabata²⁰, N. Kitamura²², T. Kobayashi²¹, Y. Kondo¹⁰, Y. Kubota⁵, A. Kurihara¹⁰, S. Leblond²¹, J. Lee⁴, P. Liang⁴, H. Liu¹¹, T. Lokotko⁴, M. Marqués⁶, Y. Matsuda⁸, A. Mattha⁶, H. Miki¹⁰, T. Nakamura¹⁰, A. Obertelli¹¹, N. Orr⁶, H. Otsu⁵, V. Panin⁵, E. Rindel¹, M. Sasano⁵, T. Shimada¹⁰, A.I. Stefanescu^{15,16}, L. Stuhl⁸, Y. Sun¹¹, D. Suzuki⁵, J. Tanaka⁵, Y. Togano⁹, T. Tomai¹⁰, L. Trache¹⁵, D. Tudor^{15,16}, T. Uesaka⁵, H. Wang⁵, X.X. Xu^{3,4}, H. Yamada¹⁰, Z.H. Yang^{5,18}, M. Yasuda¹⁰, and J. Zenihiro^{5,7}

¹Université Paris-Saclay, CNRS/IN2P3, IJCLab, 91405 Orsay, France

²Key Laboratory of Nuclear Physics and Ion-beam Application (MOE), Institute of Modern Physics, Fudan University, Shanghai 200433, China

³CAS Key Laboratory of High Precision Nuclear Spectroscopy, Institute of Modern Physics, Chinese Academy of Sciences, Lanzhou 730000, China

⁴Department of Physics, The University of Hong Kong, Hong Kong, China

⁵RIKEN Nishina Center, 2-1 Hirosawa, Wako, Saitama 351-0198, Japan

⁶LPC Caen, ENSICAEN, Université de Caen, CNRS/IN2P3, F-14050 Caen Cedex, France

⁷Cyclotron and Radioisotope Center (CYRIC), Tohoku University, Sendai 980-8578, Japan

⁸Center for Nuclear Study, University of Tokyo, RIKEN Campus, Wako, Saitama 351-0198, Japan

⁹Department of Physics, Rikkyo University, 3-34-1 Nishi-Ikebukuro, Toshima, Tokyo 171-8501, Japan

¹⁰Department of Physics, Institute of Science Tokyo, 2-12-1 O-Okayama, Meguro, Tokyo 152-8551, Japan

¹¹Institut für Kernphysik, Technische Universität Darmstadt, 64289 Darmstadt, Germany

¹²GSI Helmholtzzentrum für Schwerionenforschung, 64291 Darmstadt, Germany

¹³Istituto Nazionale di Fisica Nucleare, Sezione di Catania, 95125 Catania, Italy

¹⁴INFN Sezione di Milano, 20133 Milano, Italy

¹⁵Horia Hulubei National Institute for R&D in Physics and Nuclear Engineering (IFIN-HH), 077125 Măgurele, Romania

¹⁶Doctoral School of Physics, University of Bucharest, Măgurele, Romania

¹⁷IRFU, CEA, Université Paris-Saclay, F-91191 Gif-sur-Yvette, France

¹⁸School of Physics and State Key Laboratory of Nuclear Physics and Technology, Peking University, Beijing 100871, China

¹⁹Department of Physics, Kyoto University, Kitashirakawa-Oiwake, Sakyo-ku, Kyoto 606-8502, Japan

²⁰Department of Physics, Osaka University, Toyonaka, Osaka 560-0043, Japan

²¹Department of Physics, Tohoku University, Sendai 980-8578, Japan

²²Center for Nuclear Study, University of Tokyo, RIKEN Campus, Wako, Saitama 351-0198, Japan

Abstract. The energy spectrum of 6-neutrons was reconstructed using a ^{14}Be beam at 150 MeV/u impinging on a solid hydrogen target to perform the $(p, p\alpha)$

*e-mail: omar.nasr@ijclab.in2p3.fr

**e-mail: Didier.Beaumel@ijclab.in2p3.fr

***e-mail: lipengjie@fudan.edu.cn

reaction, followed by the decay of ^{10}He into ^4He and six neutrons. The missing-mass method was applied to determine the ^{10}He states and their subsequent decay. A Voigt fit of the ^{10}He spectrum gated on its ^8He decay products, yielded a resonance energy of $E_r = 1.40(22)$ MeV with a width of $\Gamma = 0.88(23)$ MeV for the ground-state; A first excited states was identified at $E_r = 4.00(52)$ MeV with a width of $\Gamma = 1.49(35)$ MeV; The fit resulted in reduced χ^2 of 1.24. These preliminary values are in good agreement with previous experimental results.

1 Introduction

The study of multineutrons has started as early as the 1960s. This is primarily because the possible existence of a bound or quasi-bound state of neutrons would alter our fundamental understanding of nucleon–nucleon interactions and the physics of neutron stars [1]. From these early experiments no conclusive results could be obtained. With the advent of the 21st century and the development of radioactive ion beams (RIBs), new opportunities were open and the search was revived. The first experiment with RIBs was performed at GANIL using the breakup of a ^{14}Be beam at 35 MeV/u on a carbon target, where six events were observed in coincidence with ^{10}Be residues, compatible with the observation of a bound or quasi-bound tetraneutron [2]. Several experiments followed, aiming to investigate the $3n$ and $4n$ systems. Recently, M. Duer et al. used the SAMURAI spectrometer at RIKEN to perform a $(p, p\alpha)$ reaction experiment where a ^8He beam at 156 MeV/u bombards a hydrogen target and the excitation energy of the $4n$ system was reconstructed using the missing-mass method. A resonance-like peak was observed at $E_r = 2.37$ MeV with $\Gamma = 1.7$ MeV, followed by a broad structure at around $E \sim 30$ MeV [3]. A possible origin of the sharp near-threshold peak as suggested by Lazauskas et al. is the effect of dineutron–dineutron correlations [4]. While the origin of the observed peak remains to be clarified, we experimentally investigated the heavier 6-neutron system, the question being whether such a structure near threshold is observed in a missing mass experiment, in which the simultaneous detection of several neutrons is not required. To our knowledge, no realistic structure calculations are available to date for this very exotic system. In our approach, the production method of the $6n$ system is the decay channel $^4\text{He} + 6n$ of resonances in the unbound nucleus ^{10}He .

At the RIKEN Nishina Center, the SAMURAI12 experiment was carried out using the SAMURAI spectrometer [5]. A $(p, p\alpha)$ quasi-free scattering reaction of ^{14}Be on a solid hydrogen target in inverse kinematics was employed to populate resonances in ^{10}He and to explore its decay into $^4\text{He} + 6n$ via the missing-mass method. Since ^{10}He is unbound and both its ground state and excited states remain a subject of debate, this measurement provides valuable input. In this work, we present preliminary results on the contributions of resonances in ^{10}He and compare with previous experimental results [6, 7]. We also present the first reconstructed spectrum for the 6-neutron system produced through the decay of resonances of ^{10}He .

2 Experimental setup

To produce the secondary beams in our SAMURAI12 experiment, a primary beam of ^{18}O at 230 MeV/u with intensity 500 pA bombarded a 15-mm-thick Be target, generating three possible beam settings: $^{10,12,14}\text{Be}$ at 150 MeV/u. For the ^{10}He and $6n$ studies, the beam of interest was the ^{14}Be beam setting with intensity of 2×10^5 pps and purity of above 90%. The secondary beam was then separated, focused and delivered onto a 2-mm-thick solid

hydrogen target (SHT) [8] using the BigRIPs fragment separator [9] to induce the $(p, p\alpha)$ reaction, which produces ^{10}He in the exit channel. The beam particles were identified on an event-by-event basis using the $\Delta E - \text{ToF}$ method. The energy and PID utilized the energy loss at plastic scintillators located at the focal point F13 at the entrance of the experimental hall of the SAMURAI spectrometer while the ToF was determined using the difference between the time signals of the focal planes F7 and F13. The beam profile and angle of incidence on the target were measured using two drift chambers placed upstream from the target (Beamline DC).

A schematic representation of the SAMURAI12 experimental setup is shown in Fig. 1. The recoil protons of the $(p, p\alpha)$ reaction were detected using the recoil protons spectrometer (ESPRI), which covered angles from $50^\circ - 70^\circ$ in the lab frame. As shown in Fig. 1, ESPRI consists of two arms, each containing a drift chamber for measuring the scattering angle, a large area plastic scintillator, and NaI(Tl) scintillators for energy determination [10, 11]. The emitted alpha particles were detected using two sets of telescopes, which cover angles from $4^\circ - 14^\circ$ in the lab frame. Each set consists of double-sided silicon strip detectors (DSSD) used to measure energy loss and scattering angle, and CsI(Tl) detectors for full energy reconstruction [10].

Downstream the target chamber, a drift chamber (FDC0) located before the entrance of the SAMURAI magnet was used to determine the scattering angle of the ^{10}He decay products (^{10}He decays instantly). A second, larger drift chamber (FDC2), positioned after the magnet, detected the outgoing alpha particles enabling $B\rho$ calculation to determine their energy. Residual particles identification was performed using two large walls of plastic scintillators called Hodoscope (HODF-HODP) placed behind FDC2. In addition, two walls of neutron scintillation detectors called NEBULA were employed for background suppression.

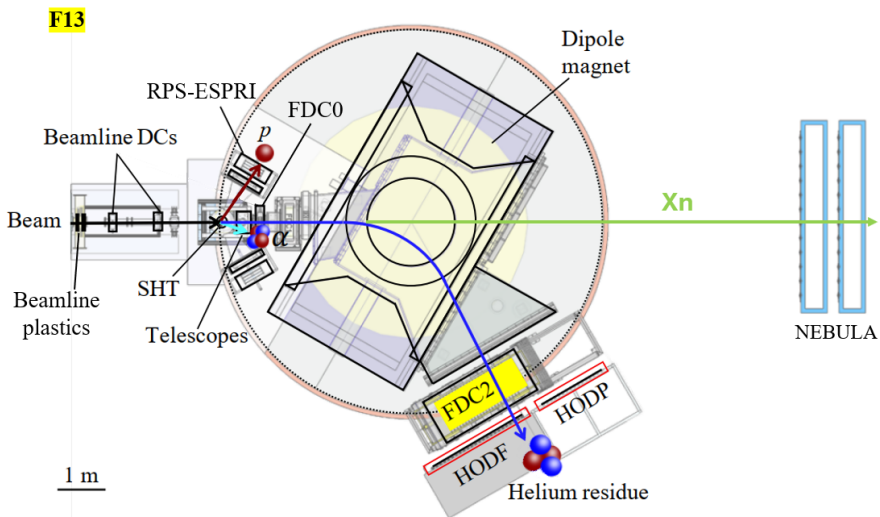


Figure 1. SAMURAI12 experimental setup. Refer to text for detailed description.

3 Analysis and Results

The selection of events for the extraction of the ^{10}He energy spectrum was carried out in three main steps: identification of the beam, recoil protons, and scattered alpha particles from the $(p, p\alpha)$ reaction. For the analysis of the 6-neutrons events, an additional step was required to determine the energy of the decay alpha through $B\rho$ reconstruction using the SAMURAI magnet field map, and data of the FDC0 and FDC2 detectors while using NEBULA as a trigger.

The identification of the ^{14}Be beam was first performed using the plastic beamline scintillators. An energy spread of the ^{14}Be beam was observed due to the wide momentum slits opening used to achieve high beam intensity. The recoil protons were then detected with the ESPRI system, where both the scattering angle and energy were measured. The proton energy was initially obtained using the $\Delta E - E$ method. However, it was later found that employing the ESPRI plastic ToF improved the statistics by nearly a factor of two due to limited geometrical acceptance of the NaI(Tl) detectors. Additionally, the recovery of events with low energy (lower than 25 MeV, the punch-through energy of protons in the ESPRI plastic detector) was possible. Therefore, this method was adopted for the analysis.

The scattered alpha particles were identified with the Telescope system. The DSSD detectors were calibrated using the self-calibration method (SCM) [12], while the CsI(Tl) detectors were calibrated with a de-focused alpha beam of ~ 157 MeV/u. The residue nuclei of the $(p, p\alpha)$ reaction and decay of ^{10}He were identified using the energy-loss and time-of-flight, measured by the hodoscope (HODF and HODP) as shown in Fig.2.

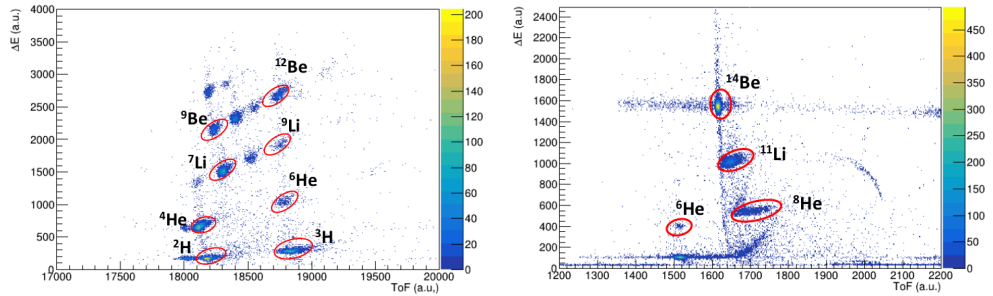


Figure 2. Hodoscope particle identification for a single bar. HODF(left), HODP(right).

3.1 ^{10}He excitation energy

To deduce the energy of ^{10}He , the standard conservation of energy and momentum relations were applied. From these equations, the momentum of ^{10}He was obtained (equation 1) and its energy deduced (equation 2) with the ^{10}He energy spectrum obtained from equation 3.

$$P_{^{10}\text{He}} = \sqrt{P_{^{14}\text{Be}}^2 + P_p^2 + P_\alpha^2 - 2P_{^{14}\text{Be}}P_p\cos\theta_p - 2P_{^{14}\text{Be}}P_\alpha\cos\theta_\alpha + 2P_pP_\alpha\cos\theta_{p-\alpha}} \quad (1)$$

$$E_{^{10}\text{He}} = E_{^{14}\text{Be}} + E_H - E_p - E_\alpha \quad (2)$$

$$E^*(^{10}\text{He}) = \sqrt{E_{^{10}\text{He}}^2 - P_{^{10}\text{He}}^2} - m_{^8\text{He}+2n} \quad (3)$$

Different gates on the residues detected in SAMURAI were applied to extract the corresponding spectra of ^{10}He , in particular the ^8He and ^4He gates obtained from HODF and HODP respectively. Figure 3 shows the ^{10}He energy spectrum relative to $^8\text{He} + 2n$ threshold, in coincidence with both ^8He and ^4He decay products. The spectrum gated by ^6He residues was not presented as most of the ^6He nuclei were lost in the gap between HODF and HODP. As shown in Fig.3, ^8He decay channel is dominant, even at energies above $^4\text{He} + 6n$ decay threshold (3.1 MeV). We also note the rather flat shape of the alpha-gated spectrum in the negative energy part, which indicates the presence of a sizable background.

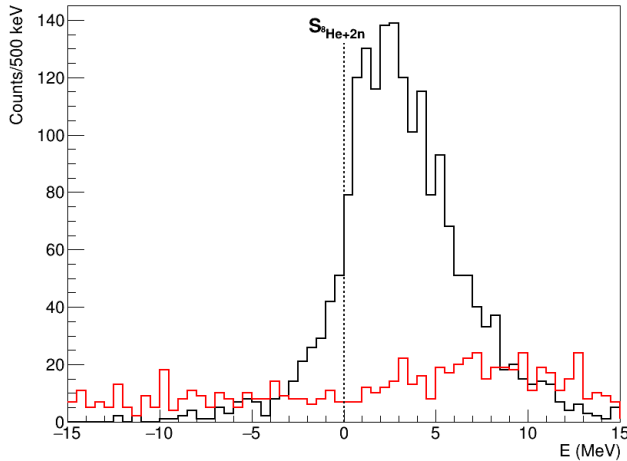


Figure 3. ^{10}He energy relative to $^8\text{He} + 2n$ gated by ^8He in black and ^4He in red.

To fit the energy spectrum gated by ^8He and extract the contributions of resonances in ^{10}He , the Voigt function (convolution of a Gaussian and a Breit–Wigner distribution) was employed.

$$F_{\text{voigt}}(E) = \int_{-\infty}^{+\infty} dE' \cdot F_{\text{Gauss}} \cdot F_{\text{BW}} \quad (4)$$

The Gaussian component was determined from the experimental data of the $^{12}\text{Be}(p, p\alpha)^8\text{He}$ reaction for which the excitation energy spectrum is just a single peak representing the ground-state transition. In a first step, the sigma was taken as constant in the fits ($\sigma = 1.37$ MeV). For the Breit–Wigner distribution, the energy-dependent width Γ followed the form [7]:

$$\Gamma(E) = \frac{2\gamma_0}{(\pi M \rho_{ch}^2) [J_{k+2}^2(\chi \rho_{ch}) + N_{k+2}^2(\chi \rho_{ch})]} \quad (5)$$

where $\chi = \sqrt{2ME}$ and ρ_{ch} is the penetrability of the decay channel, fixed at 40 fm, M is the nucleon mass and K the hyper momentum of the neutron pair while J and N are the regular and irregular Bessel functions, respectively, and γ_0 is the reduced width (free parameter).

The missing mass spectrum of ^{10}He gated by ^8He was fit with two resonances, leaving the width and mean values of energy as free parameters. A third resonance previously observed in [7] was included in the fit using the fixed energy $E_r(2) = 6.3$ MeV but it did not improve significantly the Chi2. The result of the fit, shown in Fig.4, identifies a resonance at $E_r(g.s.) = 1.40(22)$ MeV with a width of $\Gamma = 0.88(23)$ MeV, which is assigned to the ^{10}He ground

state, consistent with $^{11}\text{Li}(-1p)$ studies e.g. [6, 7] though with a smaller width. A second resonance, corresponding to the first excited state, was found at $E_r = 4.00(52)$ MeV with $\Gamma = 1.49(35)$ MeV. The overall fit yielded a reduced Chi2 of = 1.24, in good agreement with previous work[6].

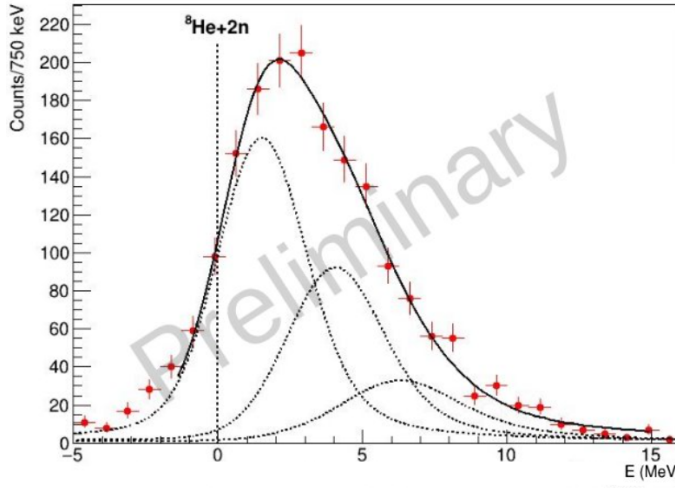


Figure 4. ^{10}He energy spectrum from $^{14}\text{Be}(p, p\alpha)^{10}\text{He}$ reaction w.r.t $^8\text{He} + 2n$ fit with Voigt function.

3.2 6-neutrons spectrum from the decay of ^{10}He resonances

The energy of the 6-neutron system, relative to the combined mass of six free neutrons, was reconstructed using the following relations:

$$P_{6n} = \sqrt{P_{^{10}\text{He}}^2 + P_{\alpha}^2 - 2P_{^{10}\text{He}}P_{\alpha}\cos\theta_{^{10}\text{He}-\alpha}} \quad (6)$$

$$E_{6n} = E_{^{10}\text{He}} - E_{\alpha} \quad (7)$$

$$E^*(6n) = \sqrt{E_{6n}^2 - P_{6n}^2} - 6m_n \quad (8)$$

The B_p value of these ^4He residues was calculated using NPTOOL [13] with the measured positions before and after the magnet, determined with FDC0 and FDC2, respectively, and the SAMURAI field map as inputs.

The ^{10}He spectrum gated by alpha residues is shown in Fig.5 [Left]. The spectrum filtered by the condition of the neutron wall NEBULA being hit (by setting a gate on the trigger parameter) is displayed as the red histogram while the spectrum in black does not utilize the NEBULA trigger. With this latter filter, one observes a stronger reduction of the counts at negative energy than in the region (in shaded blue) where the emission of several neutrons is expected. It indicates that this filter reduces background.

The 6-neutrons spectrum obtained using equation 8 by plotting events corresponding to ^{10}He energies in the energy range 0-15 MeV is shown in Fig.5 [right], with and without the NEBULA trigger (red and black histograms respectively). This first spectrum does not provide evidence for a near-threshold structure, as it reflects the ^{10}He decay integrated over

a broad energy range, including low energies that can only feed the low-energy region of the $6n$ spectrum. Concerning the negative energy part, corresponding to the bound-state region, counts are observed. It is expected that background is contributing to the spectrum over the plotted range.

The data analysis is presently continuing in order to reduce the background by e.g. using the backtracking method where data from the drift chambers of ESPRI are used to obtain the vertex of the reaction. Indeed the beam crosses several windows and air upstream and downstream the target before entering SAMURAI. Furthermore, detailed simulations are undergoing to deduce the energy resolution in the 6-neutrons spectrum.

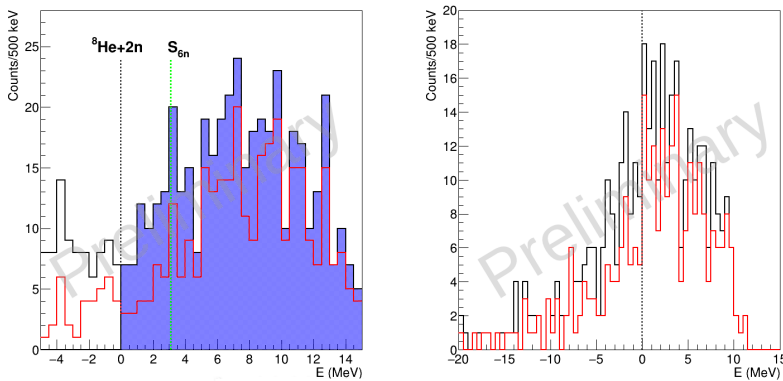


Figure 5. ^{10}He energy w.r.t $^8\text{He} + 2n$ with shaded area representing energy range used for $6n$ spectrum (Left). $6n$ spectrum (Right). See text.

4 Conclusion

To summarize, the first 6-neutrons energy spectrum was obtained using the decay of resonances in ^{10}He produced via the quasi-free scattering reaction of ^{14}Be on a solid hydrogen target $^{14}\text{Be}(p, p\alpha)^{10}\text{He}$. Neutron detectors were utilized to reduce the background. The $B\rho$ calculation of the decay alpha was used to determine the energy of the 6-neutron system. While counts are observed below the decay threshold, the low statistics and significant background prevent any firm conclusions. Further analysis to reduce background and precisely determine the energy resolution is required. The analysis of the ^{10}He spectra confirmed the presence of its ground state and low-lying excited states with energies and widths that are compatible with previous studies.

References

- [1] F.M. Marqués, Eur. Phys. J. Plus **136**, 594 (2021)
- [2] F.M. Marqués *et al.*, Phys. Rev. C **65**, 044006 (2002)
- [3] M. Duer, T. Aumann, R. Gernhäuser *et al.*, Nature **606**, 678 (2022)
- [4] R. Lazauskas, E. Hiyama, J. Carbonell, Phys. Rev. Lett. **130**, 102501 (2023)
- [5] T. Kobayashi *et al.*, Nucl. Instrum. Methods Phys. Res. B **317**, 294 (2013)
- [6] H.T. Johansson *et al.*, Nucl. Phys. A **842**, 15 (2010)

- [7] A. Matta *et al.*, Phys. Rev. C **92**, 041302(R) (2015)
- [8] Y. Matsuda *et al.*, Nucl. Instrum. Methods Phys. Res. A **643**, 6 (2011)
- [9] T. Kubo, Nucl. Instrum. Methods Phys. Res. B **204**, 97 (2003)
- [10] P.J. Li *et al.*, Phys. Rev. Lett. **131**, 212501 (2023)
- [11] Y. Matsuda *et al.*, Phys. Rev. C **87**, 034614 (2013)
- [12] R. Qiao *et al.*, IEEE Trans. Nucl. Sci. **61**, 596 (2014)
- [13] A. Matta *et al.*, J. Phys. G **43**, 045113 (2016)